

Article

Applications of Copolymers Consisting of 2,6-di(9H-carbazol-9-yl)pyridine and 3,6-di(2-thienyl)carbazole Units as Electrodes in Electrochromic Devices

Chung-Wen Kuo ¹, Jui-Cheng Chang ², Yu-Ting Huang ¹, Jeng-Kuei Chang ³ , Li-Ting Lee ⁴ and Tzi-Yi Wu ^{5,*} 

¹ Department of Chemical and Materials Engineering, National Kaohsiung University of Science and Technology, Kaohsiung 80778, Taiwan; welly@nkust.edu.tw (C.-W.K.); a3473179@gmail.com (Y.-T.H.)

² Bachelor Program in Interdisciplinary Studies, National Yunlin University of Science and Technology, Yunlin 64002, Taiwan; d700215@gmail.com

³ Department of Materials Science and Engineering, National Chiao Tung University, Hsinchu 30010, Taiwan; jkchang@nctu.edu.tw

⁴ Department of Materials Science and Engineering, Feng Chia University, Taichung 40724, Taiwan; lilee@fcu.edu.tw

⁵ Department of Chemical Engineering and Materials Engineering, National Yunlin University of Science and Technology, Yunlin 64002, Taiwan

* Correspondence: wuty@gmail.yuntech.edu.tw

Received: 14 March 2019; Accepted: 12 April 2019; Published: 16 April 2019



Abstract: A series of carbazole-based polymers (PdCz, P(dCz2-co-dTC1), P(dCz2-co-dTC2), P(dCz1-co-dTC2), and PdTC) were deposited on indium tin oxide (ITO) conductive electrodes using electrochemical polymerization. The as-prepared P(dCz2-co-dTC2) displayed a high ΔT (57.0%) and multichromic behaviors ranging from yellowish green, greenish gray, gray to purplish gray in different redox states. Five organic electrochromic devices (ECDs) were built using dCz- and dTC-containing homopolymers and copolymers as anodic materials, and poly(3,4-(2,2-dimethylpropylenedioxy)thiophene) (PProdot-Me₂) as the cathodic material. The P(dCz2-co-dTC2)/PProdot-Me₂ ECD presented remarkable electrochromic behaviors from the bleached to colored states. Moreover, P(dCz2-co-dTC2)/PProdot-Me₂ ECD displayed a high optical contrast (ΔT , 45.8%), short switching time (ca. 0.3 s), high coloration efficiency (528.8 cm² C⁻¹) at 580 nm, and high redox cycling stability.

Keywords: copolymer; electrochromic material; spectroelectrochemistry; coloration efficiency; electrochromic device; redox stability

1. Introduction

Over the past numerous years, several inorganic and organic electrochromic materials have been extensively studied for use in the rear-view mirrors of vehicles, displays, helmet visors, and windows of buildings [1]. In these electrochromic materials, reversible redox reactions lead to an important change in transmitted (or reflected) light. The promising inorganic electrochromic materials are transition metal oxides (e.g., WO₃, Ta₂O₅, TiO₂, Nb₂O₅, and MoO₃), whereas the potential organic electrochromic materials are π -conjugated polymers, viologen derivatives, metallophthalocyanines, and metallopolymers [2]. Among these organic electrochromic materials, recent research has concentrated interest on the applications of conjugated polymers as electrochromic (EC) electrodes due to their fast-electrochromic switching time [3], satisfactory coloration efficiency [4], and wide color availability through the chemical structures modification [5]. The organic EC

materials are particularly polyaniline [6], polytriphenylamine [7], polyindole [8], polycarbazole [9], polypyrrole [10], polythiophene [11], polyselenophene [12], poly(3,4-ethylenedioxythiophene) (PEDOT) [13], and polyanthracene [14]. Polytriphenylamine, polycarbazole and their derivatives have been broadly used for numerous optical and electrochemical devices due to their good hole-transporting/mobile abilities and high thermal stability [15,16]. The redox peaks and electrochromic behaviors of polytriphenylamine and polycarbazole depend on the types and number of substituents, which contain electron-donating and electron-withdrawing units. Ak et al. reported on the electrochromic behaviors of a carbazole based star shaped polymer (PTPC). The PTPC displayed absorption peaks at 308, 460, and 780 nm, which are in agreement with the π - π^* transition peak, polaron band, and bipolaron band of the PTPC, respectively. The PTPC film was green in its oxidized state and transparent in its reduced state [17]. Zhang et al. reported the preparation and electrochromic characterizations of a triphenylamine-, carbazole-, and EDOT-containing electrochromic copolymer film (P(CDPN-co-EDOT)) [18]. The P(CDPN-co-EDOT) film displayed four kinds of colors (claret red, green, cadetblue, and blue) from the neutral state to the oxidized state. The ΔT of P(CDPN-co-EDOT) was 36% and 43% in visible zone and near-IR region, respectively. Polythiophene and its derivatives are widely studied owing to their interesting characteristics such as narrow band gaps and desirable stability in air [19]. However, the onset oxidation potentials of polythiophene films are high [20]. Reynolds et al. synthesized the EDOT analogs such as 3,4-propylenedioxythiophene (ProDOT) and EDOT-Me and investigated the electrochromic properties of their corresponding PProDOT and PEDOT-Me polymer films, which displayed lower onset oxidation potentials than those of polythiophene films. The ΔT of these PEDOT derivatives were 44–63% at ca. 590 nm [21]. Since PProDOT film displays no significant absorption band in UV-Vis zone in oxidized state and the color is dark blue in reduced state, PProDOT is a potential cathodic material of electrochromic devices (ECDs). Moreover, vapor phase polymerization (VPP) and oxidative chemical vapor deposition (oCVD) are also widely used in synthesis of conjugated polymers [22,23].

In the present study, two homopolymers (PdCz and PdTC) and three copolymers (P(dCz2-co-dTC1), P(dCz2-co-dTC2), P(dCz1-co-dTC2)) with different dCz/dTC feed molar ratios were electrosynthesized to study their potential applications in ECDs. 2,6-di(9H-carbazol-9-yl)pyridine unit comprises two carbazole groups linked by a pyridine core, such donor-acceptor-donor (D-A-D) configuration is efficient for narrowing the band gap of polymers. Moreover, two carbazole groups in each repeat unit of polymer backbone facilitate the formation of radical cations and dication upon oxidation. In addition, the chemical structure of 3,6-di(2-thienyl)carbazole group displays that a carbazole unit inserts between two thiophene units, PdTC is easier to oxidize due to the donor capability of the carbazole. Poly(3,6-carbazole) has been shown to have a short conjugation length. The incorporation of thiophenes at 3,6-positions of carbazole unit would extend this conjugation length, leading to low oxidation potentials. Furthermore, five ECDs consisted of PdCz, P(dCz2-co-dTC1), P(dCz2-co-dTC2), P(dCz1-co-dTC2), or PdTC as the anodic material, and PProdot-Me₂ as the cathodic material were fabricated and their spectroelectrochemical characteristics, transmittance-time profiles, and long-term electrochemical stability were studied in detail.

2. Experimental

2.1. Materials

2,6-di(9H-carbazol-9-yl)pyridine (dCz), 3,6-di(2-thienyl)carbazole (dTC), and Prodot-Me₂ were prepared according to previously published methods [24,25]. Electrolytes of electrochromic devices were prepared using poly(methyl methacrylate) (PMMA):propylene carbonate (PC):LiClO₄ in a weight ratio of 33:53:14 [26].

2.2. Electrochemical Preparation of PdCz, P(dCz2-co-dTC1), P(dCz2-co-dTC2), P(dCz1-co-dTC2), PdTC, and PProdot-Me₂ Films

The electrosynthesis of PdCz, P(dCz2-co-dTC1), P(dCz2-co-dTC2), P(dCz1-co-dTC2), and PdTC films were carried out in an 0.2 M LiClO₄/acetonitrile (ACN)/dichloromethane (DCM) (1:1, by volume) solution, and the feed ratio of species for anodic polymer films were listed in Table 1. The carbazole-based polymer films were electrodeposited potentiodynamically by sweeping voltages in a range of 0.0–1.4 V (vs. Ag/AgNO₃) for 3 cycles. The Ag/AgNO₃ electrode was calibrated using ferrocene. PProdot-Me₂ film was electrodeposited potentiostatically at 1.0 V (vs. Ag/AgNO₃). Polymeric thicknesses at the electrode surfaces obtained from an Alpha-Step profilometer (KLA Tencor D-120, Milpitas, CA, USA) were about 180–300 nm.

Table 1. Feed species and molar ratio of anodic polymer electrodes (a)–(e).

Electrodes	Anodic Polymer	Feed Species of Anodic Polymer	Feed Molar Ratio of Anodic Polymer
(a)	PdCz	2 mM dCz	Neat dCz
(b)	P(dCz2-co-dTC1)	2 mM dCz + 1 mM dTC	2:1
(c)	P(dCz2-co-dTC2)	2 mM dCz + 2 mM dTC	2:2
(d)	P(dCz1-co-dTC2)	1 mM dCz + 2 mM dTC	1:2
(e)	PdTC	2 mM dTC	Neat dTC

2.3. Fabrication of Electrochromic Devices

ECDs were constructed using PdCz, P(dCz2-co-dTC1), P(dCz2-co-dTC2), P(dCz1-co-dTC2), or PdTC film as the anodic layer and PProdot-Me₂ film as the cathodic layer. The active areas of anode and cathode were 1.5 cm². The ECDs were built by arranging the reduced and oxidized polymeric films to face each other, and they were isolated by a PMMA/PC/ACN/LiClO₄ composite electrolyte.

2.4. Characterizations of Polymer Films and ECDs

The as-prepared polymer films and ECDs were characterized using a CHI627D electrochemical analyzer (CH Instruments, Austin, TX, USA) and an Agilent Cary 60 UV-Visible spectrophotometer (Varian Inc., Walnut Creek, CA, USA). The system of electrochemical experiments was implemented in a three-constituent cell. The working electrode was an ITO coated glass plate, the counter electrode was a platinum wire, and an Ag/AgNO₃ electrode was used as the reference electrode. Spectroelectrochemical experiments were monitored using a spectrophotometer, the spectroelectrochemical characterizations of polymer films were performed in a UV quartz cuvette cell (Varian Inc., Walnut Creek, CA, USA), and the path length of cell was 1 cm.

3. Results and Discussion

3.1. Electrochemical Polymerization and FT-IR Characterization

Figure 1 displays the cyclic voltammograms (CV) of 2 mM dCz, 2 mM dTC, and their mixtures (2 mM dCz + 1 mM dTC; 2 mM dCz + 2 mM dTC; 1 mM dCz + 2 mM dTC) in 0.2 M LiClO₄/ACN/DCM solution in the potential range from 0.0 to 1.4 V. The scan rate was 100 mV s⁻¹. When the number of CV cycles increased, the current density of redox peaks increased with an increasing scanning number, implying the growth of polymer films on ITO surfaces [27]. As displayed in Figure 1a, the 1st and 2nd oxidation peaks of PdCz at ca. 0.87 and 1.30 V (vs. Ag/AgNO₃), respectively, can be ascribed to the presence of radical cation and dication in a dCz unit. The CV curves of PdTC show an oxidation and a reduction peaks at 1.05 and 0.37 V, respectively, as shown in Figure 1e. The electrochemical redox peaks of PdCz and PdTC were quasi-reversible. When the CV curves were swept in the mixture of dCz and dTC monomers, the oxidation peaks of P(dCz2-co-dTC1), P(dCz2-co-dTC2), and P(dCz1-co-dTC2) appeared at 1.25, 1.19 and 1.15 V, respectively, and the reduction peaks of P(dCz2-co-dTC1), P(dCz2-co-dTC2), and P(dCz1-co-dTC2) located at 0.50, 0.43 and 0.39 V, respectively, as shown in Figure 1b–d. The redox

potentials and wave shapes of copolymers are different from those of homopolymers, and this is an evidence of the copolymerization of P(dCz2-co-dTC1), P(dCz2-co-dTC2), and P(dCz1-co-dTC2) films. The polymer films were further characterized using FT-IR, Figure 2 displayed the FT-IR spectra of electrochemically synthesized PdCz, P(dCz2-co-dTC1), P(dCz2-co-dTC2), P(dCz1-co-dTC2), and PdTC films. The characteristic peaks of PdCz are shown in Figure 2a. The characteristic band at 1095 cm^{-1} indicates the doping of PdCz film with the ClO_4^- . The characteristic peaks at around 1600 cm^{-1} represent the aromatic $\text{C}=\text{C}$ stretching vibration. The band at 1220 cm^{-1} is related to $\text{C}-\text{C}$ formation. The peak at around 1450 cm^{-1} can be ascribed to the $\text{C}-\text{N}$ stretching of the carbazole unit [28].

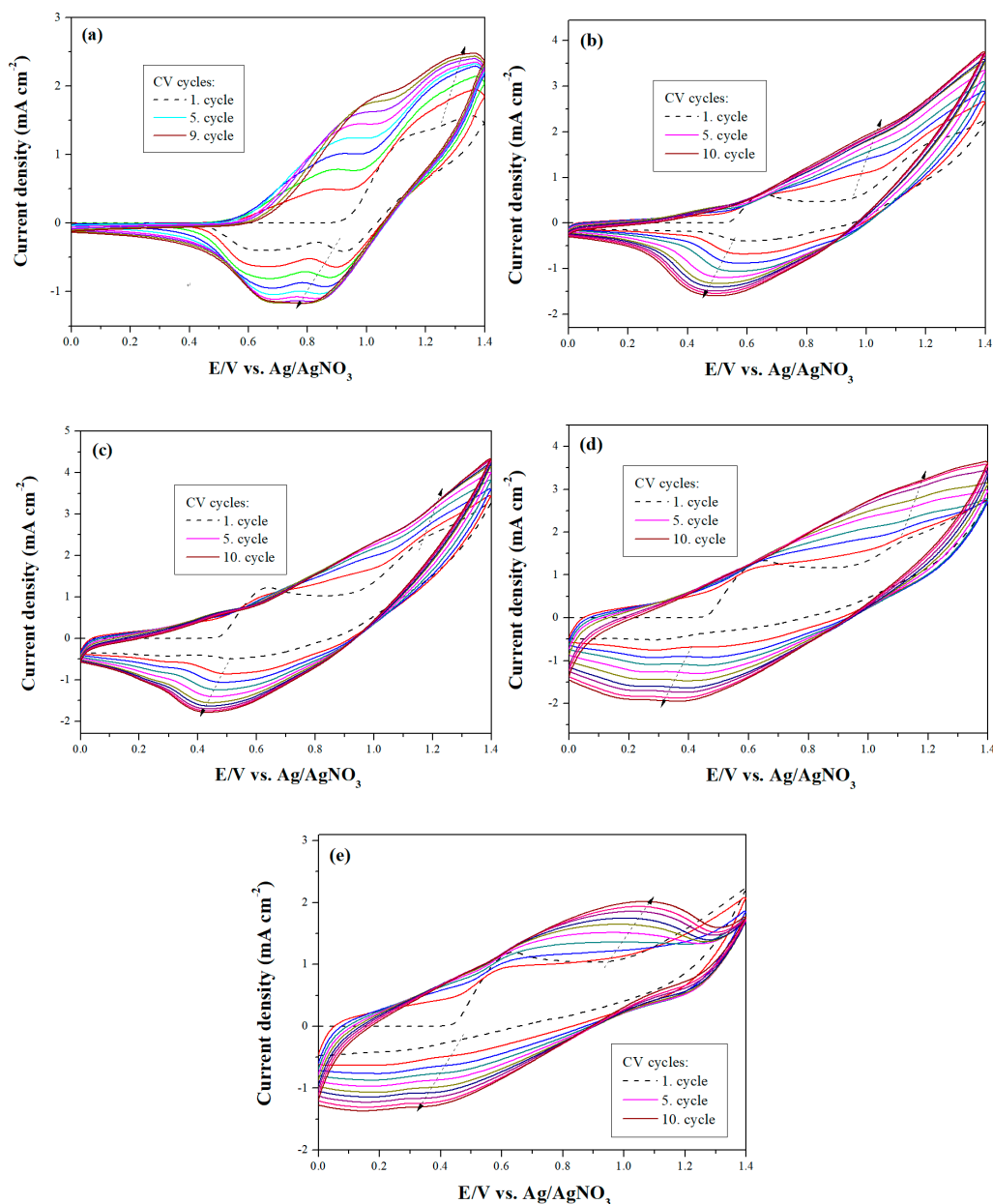


Figure 1. Electrochemical synthesis of (a) PdCz; (b) P(dCz2-co-dTC1); (c) P(dCz2-co-dTC2); (d) P(dCz1-co-dTC2) and (e) PdTC in ACN/DCM (1:1, by volume) solution at 100 mV s^{-1} on ITO working electrodes.

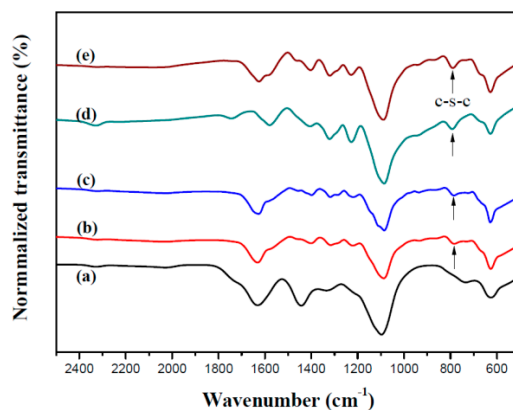


Figure 2. FT-IR spectra of (a) PdCz; (b) P(dCz2-co-dTC1); (c) P(dCz2-co-dTC2); (d) P(dCz1-co-dTC2) and (e) PdTC.

There was no conspicuous characteristic peak of PdCz at ca. 790 cm^{-1} as shown in Figure 2a. Figure 2b–d not only revealed the characteristic peaks of PdCz but also displayed the characteristic peak (-C-S-C- stretching) of PdTC, the formation of a new characteristic peak at 790 cm^{-1} could be attributed to the presence of dTC in P(dCz2-co-dTC1), P(dCz2-co-dTC2), and P(dCz1-co-dTC2) films, implying dCz- and dTC-containing copolymer films were successfully synthesized. The polymerization schemes of PdCz, P(dCz-co-dTC), and PdTC are shown in Figure 3.

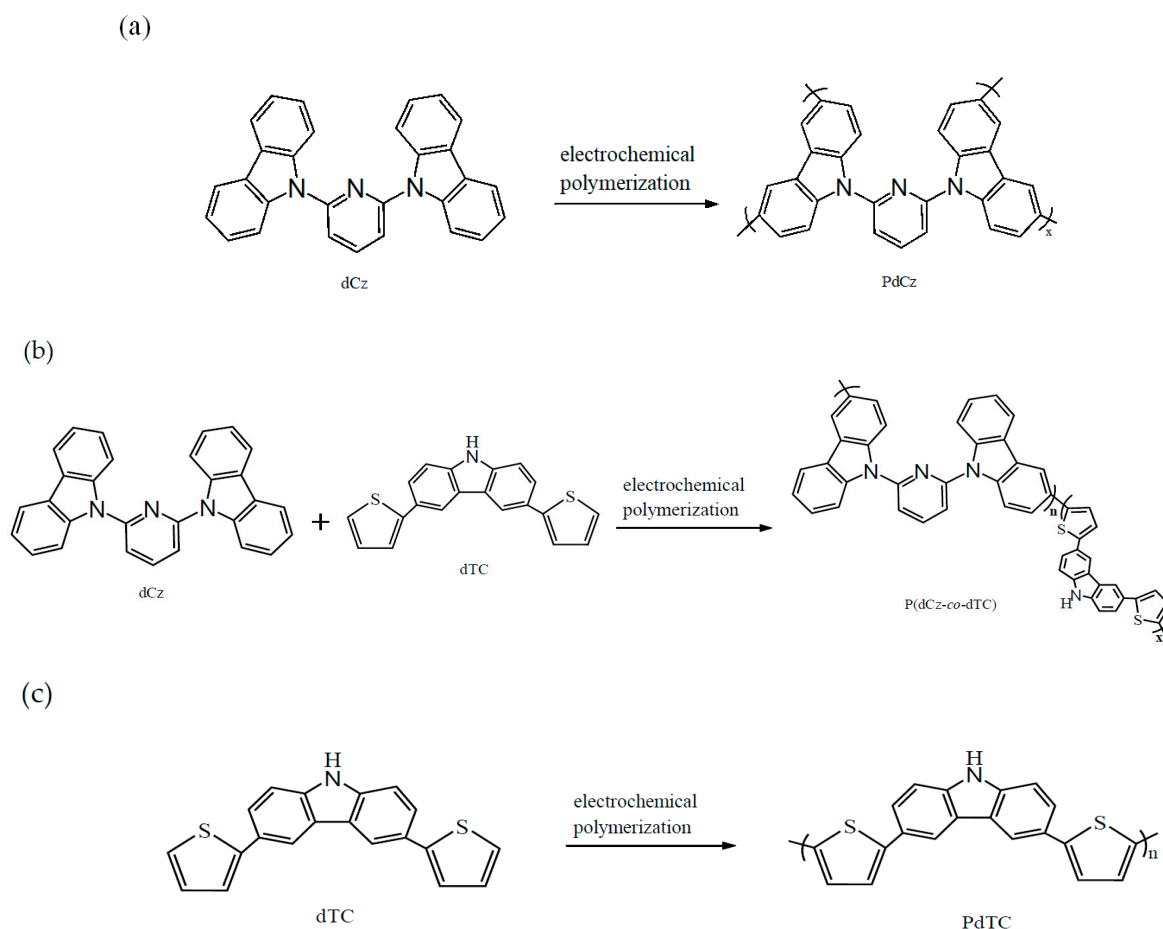


Figure 3. The electrochemical polymerization routes of (a) PdCz; (b) P(dCz-co-dTC) and (c) PdTC.

3.2. Electrochemical Properties of Polymer Films

The first rinse P(dCz2-co-dTC2) film was immersed into clean electrolyte solution, and then run in new CV curves. The as-prepared P(dCz2-co-dTC2) film was swept at 10, 50, 100, 150, and 200 mV s^{-1} in 0.2 M $\text{LiClO}_4/\text{ACN}/\text{DCM}$ using CV. As shown in Figure 4, the anodic and cathodic peaks of P(dCz2-co-dTC2) film showed a single quasi-reversible redox process and the anodic and cathodic peak current densities increased linearly with increasing scan rate (inset in Figure 4), implying the redox process of P(dCz2-co-dTC2) film was not a diffusion-controlled process [29].

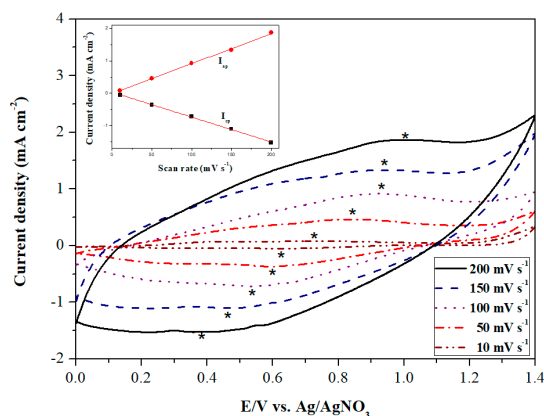


Figure 4. Cyclic voltammograms (CV) curves of the P(dCz2-co-dTC2) film at different scan rates between 10 and 200 mV s^{-1} in the $\text{LiClO}_4/\text{ACN}/\text{DCM}$ solution. Inset is scan rate dependence of the P(dCz2-co-dTC2) anodic and cathodic peak current densities.

3.3. Spectroelectrochemical Investigation of Polymer Films

Figure 5 shows UV-Visible spectra of PdCz, P(dCz2-co-dTC1), P(dCz2-co-dTC2), P(dCz1-co-dTC2), and PdTC electrodes in an ACN/DCM solution containing 0.2 M LiClO_4 . PdCz does not show distinct absorption peaks at 0.0 V but two new peaks appear at 430 and 785 nm gradually upon increasing of the applied potential, which can be attributed to the growth of charge carrier bands [30]. On the other hand, P(dCz2-co-dTC1), P(dCz2-co-dTC2), P(dCz1-co-dTC2), and PdTC electrodes display absorption peaks at 406, 410, 405, and 402 nm at 0.0 V, respectively, which can be assigned to the π - π^* transition of P(dCz2-co-dTC1), P(dCz2-co-dTC2), P(dCz1-co-dTC2), and PdTC electrodes in their reduced state. When potentials in the oxidative direction were applied, the π - π^* transition bands of P(dCz2-co-dTC1), P(dCz2-co-dTC2), P(dCz1-co-dTC2), and PdTC electrodes waned and new charge carrier bands (550 nm and 860 nm for P(dCz2-co-dTC1); 545 nm and 820 nm for P(dCz2-co-dTC2); 548 nm and 830 nm for P(dCz1-co-dTC2); 549 nm and 815 nm for PdTC) were seen at the longer wavelengths zone. The optical band gap (E_g) values of PdCz, P(dCz2-co-dTC1), P(dCz2-co-dTC2), P(dCz1-co-dTC2), and PdTC electrodes were 3.01, 2.43, 2.48, 2.42, and 2.45 eV, respectively.

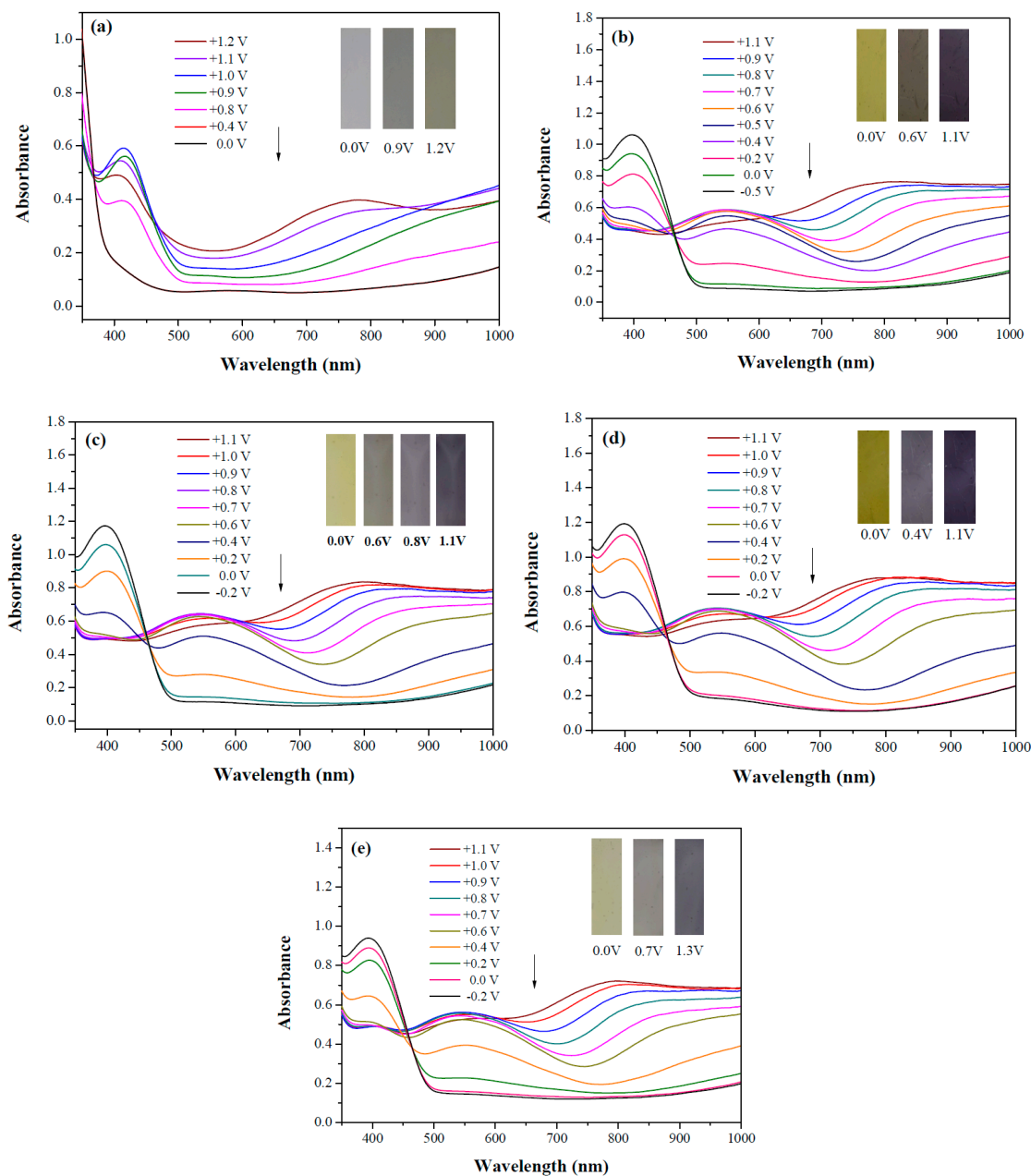
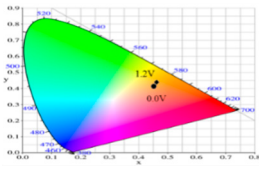
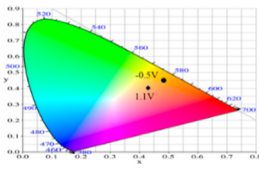
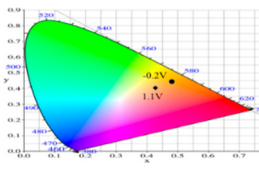
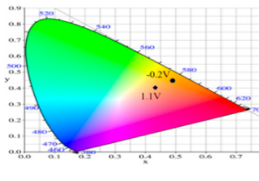
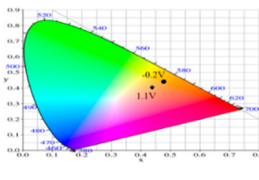


Figure 5. UV-Visible spectra of (a) PdCz; (b) P(dCz2-co-dTC1); (c) P(dCz2-co-dTC2); (d) P(dCz1-co-dTC2) and (e) PdTC electrodes on ITO in ACN/DCM (1:1, by volume) solution containing 0.2 M LiClO₄.

PdCz displayed multichromic behaviors with a light gray color in its neutral state (0.0 V), an iron grey color (0.9 V) and a dark gray color (1.2 V) during stepwise oxidation. The colors of PdTC electrode were light yellowish-gray, light gray, and iron grey at 0.0, 0.7, and 1.3 V, respectively. The dCz- and dTC-containing copolymer electrodes displayed different multichromic behaviors with PdCz and PdTC electrodes. P(dCz2-co-dTC1) film was yellowish green, gray, and purplish grey at 0.0, 0.6, and 1.1 V, respectively, whereas P(dCz2-co-dTC2) film was yellowish green, greenish gray, gray, and purplish gray at 0.0, 0.6, 0.8, and 1.1 V, respectively, and P(dCz1-co-dTC2) film was yellow, gray, and dark purplish-grey at 0.0, 0.4, and 1.1 V, respectively. The colorimetric values (L^* , a^* , and b^*), CIE (Commission Internationale de l'Éclairage) chromaticity values (x , y) and diagrams of the five polymer films at various potentials are listed in Table 2.

Table 2. Colorimetric values (L^* , a^* , and b^*), CIE chromaticity values (x , y) and diagrams of the (a) PdCz, (b) P(dCz2-co-dTC1), (c) P(dCz2-co-dTC2), (d) P(dCz1-co-dTC2), and (e) PdTC at various applied potentials.

(a)						
Potential (V)	L^*	a^*	b^*	x	y	Diagram
0.0	95.12	−0.34	2.95	0.4500	0.4106	
0.8	92.64	−1.33	18.74	0.4638	0.4258	
0.9	90.35	−1.99	25.66	0.4692	0.4328	
1.0	87.76	−3.07	23.96	0.4664	0.4334	
1.2	84.27	−4.52	18.11	0.4588	0.4311	
(b)						
Potential (V)	L^*	a^*	b^*	x	y	Diagram
−0.5	90.36	−2.48	41.83	0.4815	0.4456	
0.2	78.82	1.71	24.79	0.4775	0.4293	
0.4	64.49	5.65	1.11	0.4612	0.3999	
0.8	56.45	6.50	−7.41	0.4509	0.3859	
1.1	58.22	−2.34	−8.72	0.4284	0.3987	
(c)						
Potential (V)	L^*	a^*	b^*	x	y	Diagram
−0.2	87.82	−1.08	35.11	0.4793	0.4395	
0.2	65.75	4.92	1.02	0.4593	0.4011	
0.8	57.30	5.37	−6.45	0.4498	0.3893	
0.9	56.84	3.41	−6.98	0.4444	0.3916	
1.1	57.99	−3.38	−8.82	0.4258	0.4002	
(d)						
Potential (V)	L^*	a^*	b^*	x	y	Diagram
−0.2	85.42	0.44	42.42	0.4883	0.4432	
0.2	75.20	3.48	26.48	0.4836	0.4287	
0.6	54.48	7.37	−6.51	0.4546	0.3851	
0.9	53.03	4.21	−6.75	0.4466	0.3898	
1.1	55.04	−1.72	−7.61	0.4309	0.3990	
(e)						
Potential (V)	L^*	a^*	b^*	x	y	Diagram
−0.2	87.95	−1.58	31.51	0.4754	0.4374	
0.2	82.07	0.27	22.50	0.4719	0.4287	
0.6	65.32	5.12	−2.87	0.4543	0.3960	
0.9	61.22	5.69	−5.11	0.4525	0.3915	
1.1	61.51	−0.69	−6.32	0.4366	0.3999	

3.4. Electrochromic Switching of Polymer Electrodes

As displayed in Figure 6, PdCz, P(dCz2-co-dTC1), P(dCz2-co-dTC2), P(dCz1-co-dTC2), and PdTC films were monitored by potential stepping between neutral (0.0 V) and oxidized states (+1.1 V) with a residence time of 10 s. The ΔT values of PdCz, P(dCz2-co-dTC1), P(dCz2-co-dTC2), P(dCz1-co-dTC2),

and PdTC films were 19.7% at 790 nm, 55.7% at 790 nm, 57.0% at 784 nm, 50.6% at 790 nm, and 48.0% at 790 nm, respectively. The ΔT of P(dCz2-co-dTC1), P(dCz2-co-dTC2), and P(dCz1-co-dTC2) films were larger than those of PdCz and PdTC films in 0.2 M LiClO₄/ACN/DCM solution, indicating copolymers contain both dCz and dTC units increased ΔT significantly. The τ_c of electrodes (a), (b), (c), (d), and (e) were 4.0 s, 2.7 s, 3.5 s, 4.2 s, and 4.3 s at 3rd cycles, respectively, and the τ_b of electrodes (a), (b), (c), (d), and (e) were 0.8 s, 2.7 s, 1.8 s, 5.6 s, and 6.0 s at 3rd cycles, respectively. Different τ_c and τ_b in each set of samples may be attributed to the contact area between electrolytes and electrodes.

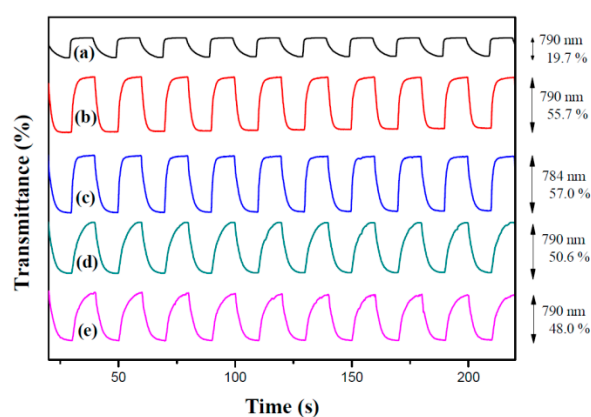


Figure 6. Optical contrast of (a) PdCz; (b) P(dCz2-co-dTC1); (c) P(dCz2-co-dTC2); (d) P(dCz1-co-dTC2) and (e) PdTC electrodes in an ACN/DCM (1:1, by volume) solution containing 0.2 M LiClO₄ with a residence time of 10 s.

ΔOD can be determined using the formula [31],

$$\Delta OD = \log\left(\frac{T_{\text{ox}}}{T_{\text{red}}}\right) \quad (1)$$

where T_{ox} and T_{red} are the transmittances in the oxidized and the reduced state, respectively.

The coloration efficiency (η) is another important parameter for practical application of polymer films in ECDs and it can be determined using the equation [32]:

$$\eta = \frac{\Delta OD}{Q_d} \quad (2)$$

where ΔOD is the discrepancy of optical density, Q_d implicates the amount of injected charges per unit electrode area. The η values of PdCz, P(dCz2-co-dTC1), P(dCz2-co-dTC2), P(dCz1-co-dTC2), and PdTC films are 81.4 cm² C⁻¹ at 790 nm, 99.3 cm² C⁻¹ at 790 nm, 248.4 cm² C⁻¹ at 784 nm, 145.3 cm² C⁻¹ at 790 nm, and 164.9 cm² C⁻¹ at 790 nm, respectively (Table 3). P(dCz2-co-dTC2) film presents the highest η among the five polymer films.

Table 3. Optical and electrochemical properties investigated at the selected applied wavelength for the electrodes.

Electrodes	λ (nm)	T_{ox}	T_{red}	ΔT	ΔOD	Q_d (mC cm ⁻²)	η (cm ² C ⁻¹)	τ_c (s)	τ_b (s)
PdCz	790	69.7	89.3	19.7	0.11	1.351	81.4	4.0	0.8
P(dCz2-co-dTC1)	790	18.5	73.9	55.7	0.60	6.043	99.3	2.7	2.7
P(dCz2-co-dTC2)	784	10.7	67.7	57.0	0.80	3.221	248.4	3.5	1.8
P(dCz1-co-dTC2)	790	10.9	61.4	50.6	0.75	5.163	145.3	4.2	5.6
PdTC	790	9.1	57.1	48.0	0.80	4.851	164.9	4.3	6.0

3.5. Spectroelectrochemical Investigation of ECDs

Figure 7 displays the UV-Vis spectra of dual-type PdCz/PProdot-Me₂, P(dCz2-co-dTC2)/PProdot-Me₂, and PdTC/PProdot-Me₂ ECDs at different applied potentials.

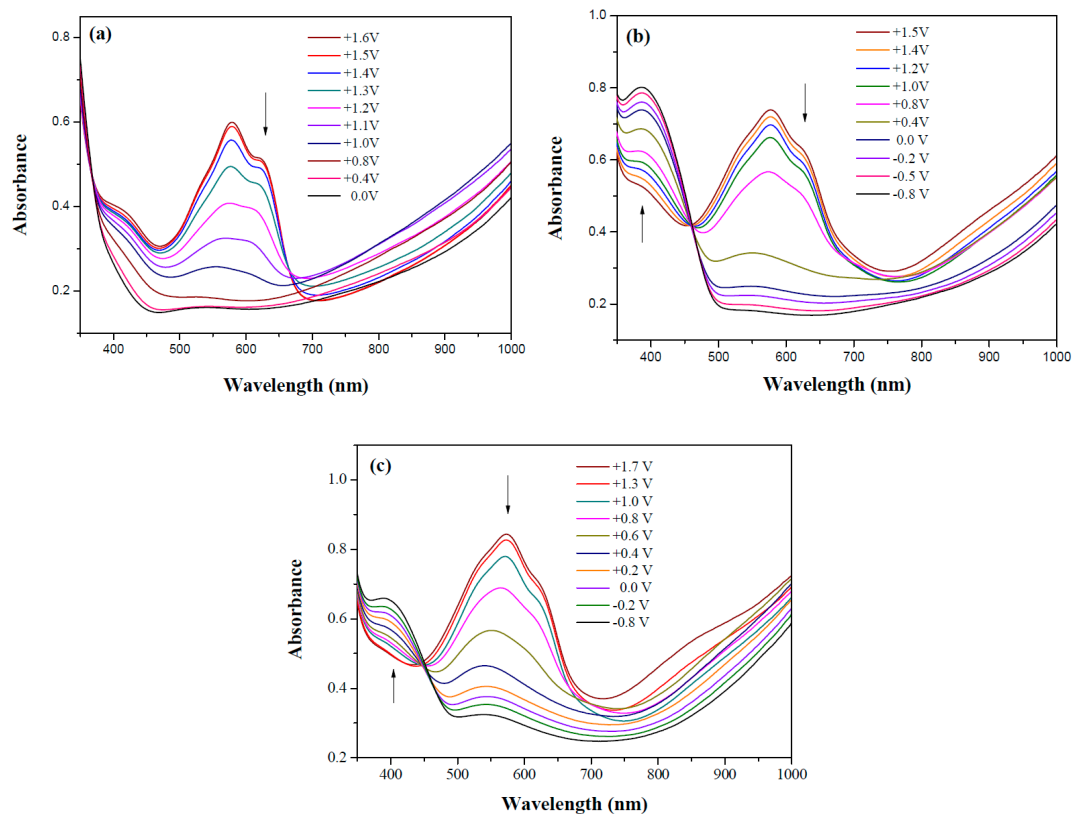


Figure 7. UV-Visible spectra of (a) PdCz/PProdot-Me₂; (b) P(dCz2-co-dTC2)/PProdot-Me₂ and (c) PdTC/PProdot-Me₂ ECDs.

PdCz/PProdot-Me₂ ECD did not show distinct absorption peaks at wavelength ranging from 350 to 450 nm at 0.0 V, P(dCz2-co-dTC2)/PProdot-Me₂ and PdTC/PProdot-Me₂ ECDs displayed distinct absorption peaks at 410 and 402 nm at 0.0 V, which could be assigned as the absorption peaks of P(dCz2-co-dTC2) and PdTC films at 0.0 V, respectively. The absorption peaks of P(dCz2-co-dTC2) and PdTC films fade with the increasing applied potential, and new absorption bands were emerged gradually at around 580 nm. This can be attributed to the stepwise reduction of PProdot-Me₂ film. The colors of PdCz/PProdot-Me₂ ECD are silver gray, gray, and purplish-gray at 0.0, 1.0, and 1.3 V, respectively. P(dCz2-co-dTC2)/PProdot-Me₂ and PdTC/PProdot-Me₂ ECDs reveal four kinds of colors from bleached to colored states. The colors of P(dCz2-co-dTC2)/PProdot-Me₂ ECD are yellowish green, iron gray, dark blue, and purplish-blue at −0.8, 0.8, 1.2, and 1.5 V, respectively. PdTC/PProdot-Me₂ ECD reveals yellowish-green, greenish-gray, grayish-blue, and purplish-blue at −0.8, 0.0, 0.8, and 1.7 V, respectively. The electrochromic photographs, colorimetric values (L^* , a^* , and b^*), CIE chromaticity values (x , y) and diagrams of PdCz/PProdot-Me₂, P(dCz2-co-dTC2)/PProdot-Me₂, and PdTC/PProdot-Me₂ ECDs at various applied potentials are listed in Table 4.

Table 4. Electrochromic photographs, colorimetric values (L^* , a^* , and b^*), CIE chromaticity values (x , y) and diagrams of the PdCz/PProdot-Me₂, P(dCz2-co-dTC2)/PProdot-Me₂ and PdTC/PProdot-Me₂ ECDs at various applied potentials.

ECDs	Potential (V)	Photographs	L^*	a^*	b^*	x	y	Diagrams
PdCz/PProdot-Me ₂	0.0		86.69	0.03	-0.06	0.4476	0.4073	
	0.8		84.93	-0.01	3.78	0.4517	0.4113	
	1.0		75.69	1.54	-3.55	0.4460	0.4013	
	1.2		67.20	0.73	-14.09	0.4290	0.3881	
	1.3		63.53	1.25	-18.88	0.4216	0.3796	
P(dCz2-co-dTC2)/PProdot-Me ₂	-0.8		85.06	-1.40	26.92	0.4724	0.4342	
	0.0		80.27	-0.28	19.04	0.4679	0.4268	
	0.8		61.82	2.72	-8.38	0.4410	0.3918	
	1.2		56.30	4.46	-17.66	0.4284	0.3737	
	1.5		54.18	5.26	-21.30	0.4229	0.3655	
PdTC/PProdot-Me ₂	-0.8		75.67	2.71	13.63	0.4686	0.4179	
	0.0		72.35	3.54	8.02	0.4644	0.4112	
	0.8		55.56	8.38	-14.34	0.4433	0.3724	
	1.3		50.05	9.67	-22.05	0.4307	0.3547	
	1.7		49.19	9.66	-22.34	0.4298	0.3535	

3.6. Electrochromic Switching of ECDs

As displayed in Figure 8, PdCz/PProdot-Me₂ and P(dCz2-co-dTC2)/PProdot-Me₂ ECDs were monitored by potential stepping between bleached and colored states with a residence time of 10 s. The ΔT , ΔOD , switching time, and η of PdCz/PProdot-Me₂, P(dCz2-co-dTC1)/PProdot-Me₂, P(dCz2-co-dTC2)/PProdot-Me₂, P(dCz1-co-dTC2)/PProdot-Me₂ and PdTC/PProdot-Me₂ ECDs are listed in Table 5. P(dCz2-co-dTC2)/PProdot-Me₂ ECD displays the highest ΔT , and P(dCz2-co-dTC1)/PProdot-Me₂ and P(dCz2-co-dTC2)/PProdot-Me₂ ECDs display higher ΔT and ΔOD than those of PdCz/PProdot-Me₂ and PdTC/PProdot-Me₂ ECDs, indicating that the use of copolymers (P(dCz2-co-dTC1) and P(dCz2-co-dTC2)) as the electrode materials brings about a higher ΔT at around 580 nm than those of homopolymers (PdCz and PdTC). Table 6 summarizes comparisons of ΔT with reported ECDs, P(dCz2-co-dTC2)/PProdot-Me₂ ECD shows higher ΔT than those reported for P(Bmco)/PEDOT [33], P(dNcbph)/PEDOT [34], P(tnCz1-bTp2)/PProdot-Me₂ [35], p(dNcbph-co-bth)/PEDOT [36], PtCz/PProDOT-Me₂ [37], and P(BCz-co-ProDOT)/triple-layer PEDOT-PSS ECDs [38]. The τ_c and τ_b of five ECDs in Table 5 are less than 1 s, which are shorter than those of polymer electrodes in a solution, disclosing the ECDs change color faster than the polymers in a solution during stepwise oxidation and reduction period [39].

Table 5. Optical and electrochemical properties investigated at the selected applied wavelength for the devices.

Devices	λ (nm)	T_{ox} (V ^a)	T_{red} (V ^a)	ΔT	ΔOD	Q_d (mC cm ⁻²)	η (cm ² C ⁻¹)	τ_c (s)	τ_b (s)
PdCz/PProdot-Me ₂	580	23.1 (1.5)	57.5 (-0.8)	34.4	0.396	0.781	507.0	0.2	0.2
P(dCz2-co-dTC1)/PProdot-Me ₂	580	15.1 (1.5)	55.2 (-0.8)	40.1	0.563	1.001	562.4	0.3	0.2
P(dCz2-co-dTC2)/PProdot-Me ₂	580	16.0 (1.5)	61.8 (-0.8)	45.8	0.587	1.110	528.8	0.2	0.3
P(dCz1-co-dTC2)/PProdot-Me ₂	578	36.8 (1.5)	69.0 (-0.8)	32.2	0.273	0.622	438.9	0.9	0.2
PdTC/PProdot-Me ₂	578	15.6 (1.5)	46.8 (-0.8)	31.2	0.477	1.083	440.4	0.2	0.2

^a The selected applied voltages for the devices.

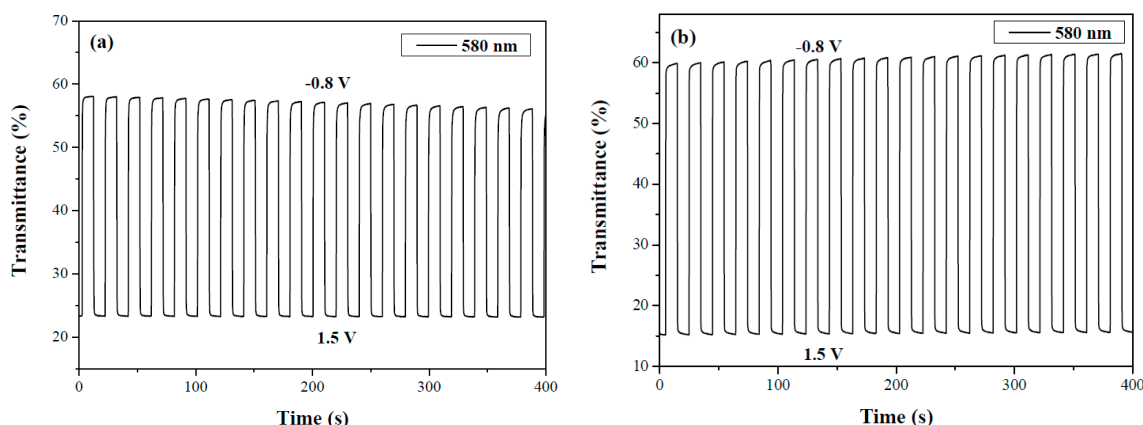


Figure 8. Optical contrast of (a) PdCz/PProdot-Me₂ and (b) P(dCz2-co-dTC2)/PProdot-Me₂ ECDs with a residence time of 10 s.

The η of PdCz/PProdot-Me₂, P(dCz2-co-dTC1)/PProdot-Me₂, P(dCz2-co-dTC2)/PProdot-Me₂, P(dCz1-co-dTC2)/PProdot-Me₂ and PdTC/PProdot-Me₂ ECDs were 507.0, 562.4, 528.8, 438.9 and 440.4 cm² C⁻¹, respectively. P(dCz2-co-dTC1) film with a dCz/dTC = 2/1 feed molar ratio presented the highest η among the five ECDs. Table 6 also summarizes comparisons of η with reported ECDs: P(dCz2-co-dTC2)/PProdot-Me₂ ECD showed higher η than those reported for p(dNcbph-co-bth)/PEDOT [36], PtCz/PProDOT-Me₂ [37], and P(BCz-co-ProDOT)/triple-layer PEDOT-PSS ECDs [38]. However, P(dCz2-co-dTC2)/PProdot-Me₂ ECD showed lower η than that reported for P(tnCz1-bTp2)/PProdot-Me₂ ECD [35].

Table 6. Optical contrast and coloration efficiencies of some ECDs.

ECD Configuration	ΔT_{\max} (%)	η (cm ² C ⁻¹)	Ref.
P(Bmco)/PEDOT	35 (620 nm)	—	[33]
P(dNcbph)/PEDOT	19 (550 nm)	—	[34]
P(tnCz1-bTp2)/PProdot-Me ₂	40 (630 nm)	539 (630 nm)	[35]
p(dNcbph-co-bth)/PEDOT	28.6 (700 nm)	234 (700 nm)	[36]
PtCz/PProDOT-Me ₂	36 (572 nm)	343.4 (572 nm)	[37]
P(BCz-co-ProDOT)/triple-layer PEDOT-PSS	41 (642 nm)	417 (642 nm)	[38]
P(dCz2-co-dTC2)/PProdot-Me ₂	45.8 (580 nm)	528.8 (580 nm)	This work

3.7. Open-Circuit Memory of ECDs

The open-circuit memory effect of PdCz/PProdot-Me₂, P(dCz2-co-dTC2)/PProdot-Me₂, and PdTC/PProdot-Me₂ ECDs was detected at bleached and colored states by applying the voltage for 1 s for each 100 s interval [40,41]. Figure 9 shows that the transmittance of the three ECDs was almost no change at the bleached state. At colored states, the three ECDs were less stable than those at bleached state. However, the loss in transmittance of ECDs at colored states was less than 4%. It is worth mentioning that P(dCz2-co-dTC2)/PProdot-Me₂ ECD showed less transmittance change at the colored state than those of PdCz/PProdot-Me₂ and PdTC/PProdot-Me₂ ECDs, disclosing that P(dCz2-co-dTC2)/PProdot-Me₂ ECD exhibited a satisfactory open-circuit memory effect.

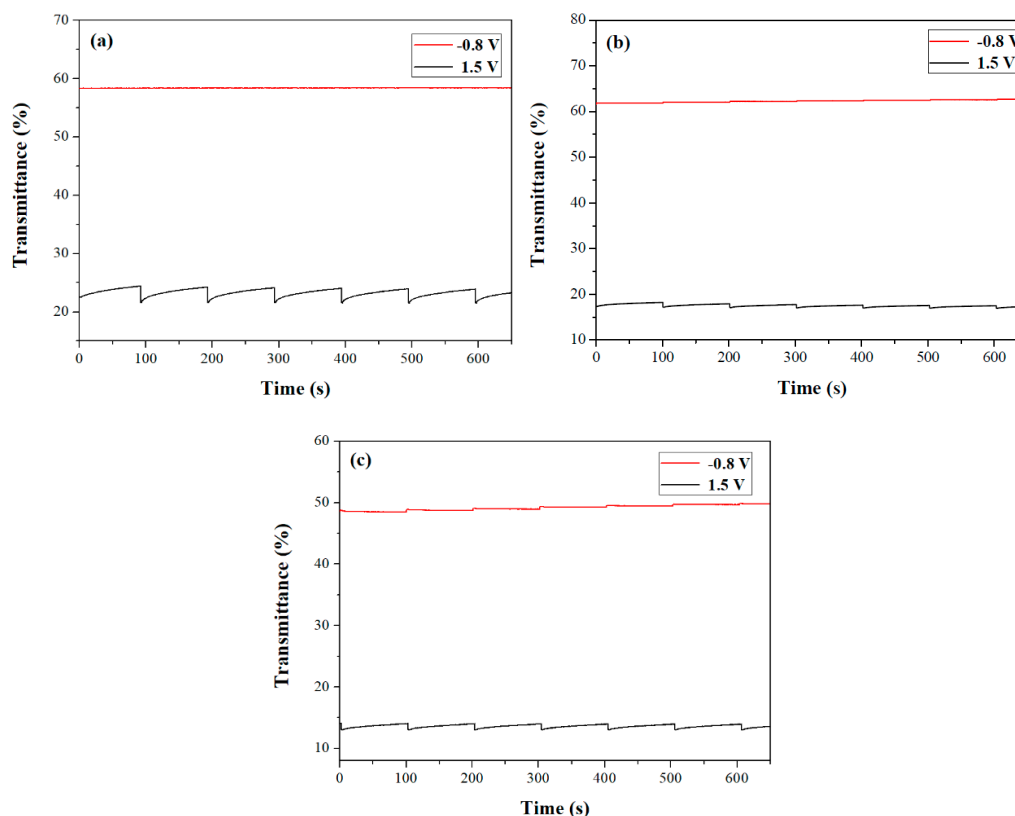


Figure 9. Open circuit stability of (a) PdCz/PProdot-Me₂; (b) P(dCz2-co-dTC2)/PProdot-Me₂ and (c) PdTC/PProdot-Me₂ ECDs.

3.8. Electrochemical Stability of ECDs

The long-term electrochemical stability of PdCz/PProdot-Me₂, P(dCz2-co-dTC2)/PProdot-Me₂, and PdTC/PProdot-Me₂ ECDs was monitored using CV at the 1st, 500th and 1000th cycles [42]. From the observation of ECDs' electrochemical ability in Figure 10, 78.4%, 95.5%, and 87.7% of electroactive stability were preserved at the 500th cycle, and 72.5%, 88.0%, and 78.2% of electroactive stability were preserved at the 1000th cycle for PdCz/PProdot-Me₂, P(dCz2-co-dTC2)/PProdot-Me₂, and PdTC/PProdot-Me₂ ECDs, respectively. P(dCz2-co-dTC2)/PProdot-Me₂ ECD showed better long-term electrochemical stability than those of PdCz/PProdot-Me₂ and PdTC/PProdot-Me₂ ECDs, disclosing the redox stability of copolymerized P(dCz2-co-dTC2) film was higher than those of homopolymerized PdCz and PdTC films and ECD employed a copolymer (P(dCz2-co-dTC2)) as anodic polymer film gave rise to a better long-term electrochemical stability than those of homopolymers (PdCz and PdTC).

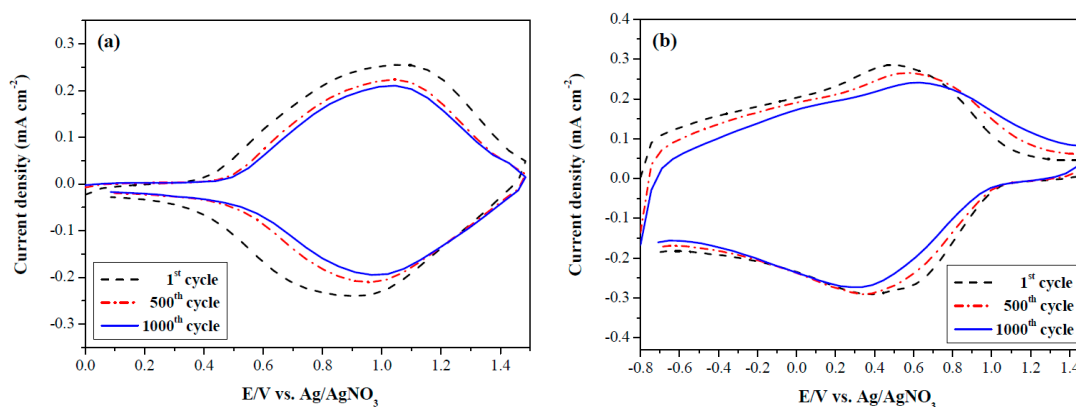


Figure 10. Cont.

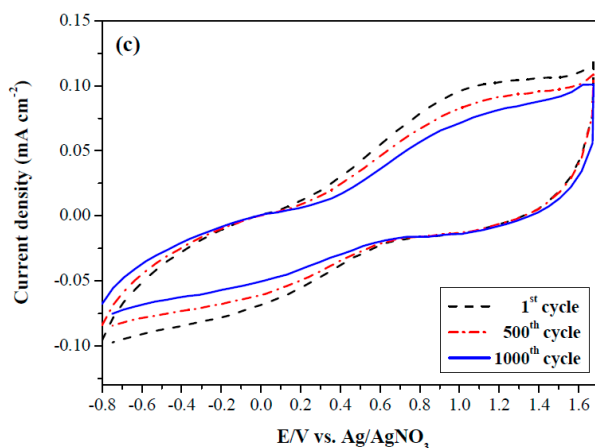


Figure 10. Cyclic voltammograms of (a) PdCz/PProdot-Me₂; (b) P(dCz2-co-dTC2)/PProdot-Me₂ and (c) PdTC/PProdot-Me₂ ECDs at a scan rate of 500 mV s⁻¹ between one and 1000 cycles.

4. Conclusions

Five ECDs' polymer electrodes (PdCz, P(dCz2-co-dTC1), P(dCz2-co-dTC2), P(dCz1-co-dTC2), and PdTC) were prepared using electrochemical copolymerization. Our experimental studies display that dCz- and dTC-containing copolymer electrodes showed multichromic behaviors and the electrochromic switching properties and coloration efficiency of the copolymers could be adjusted by various feed monomer molar ratios. P(dCz2-co-dTC1) film was yellowish green, gray, and purplish grey at 0.0, 0.6, and 1.1 V, respectively, whereas P(dCz2-co-dTC2) film was yellowish green, greenish gray, gray, and purplish gray at 0.0, 0.6, 0.8, and 1.1 V, respectively. P(dCz2-co-dTC2) film displayed a high ΔT (57.0 %) and a high η (248.4 cm² C⁻¹) at 784 nm in 0.2 M LiClO₄/ACN/DCM solution. Five ECDs based on dCz- and dTC-containing anodic polymer electrodes and PProdot-Me₂ cathodic polymer electrodes were built and electrochromic properties were characterized. P(dCz2-co-dTC2)/PProdot-Me₂ ECD exhibited a high ΔT (45.8 % at 580 nm) and high long-term electrochemical stability, whereas P(dCz2-co-dTC1)/PProdot-Me₂ ECD exhibited high η (562.4 cm² C⁻¹ at 580 nm) and a rapid switching time (≤ 0.3 s). In view of the above studies, dCz- and dTC-containing copolymers are amenable for use in ECDs.

Author Contributions: C.-W.K. conceived the research topic. Y.-T.H., J.-C.C., and T.-Y.W. carried out the experiments. C.-W.K., T.-Y.W., J.-C.C., L.-T.L., and J.-K.C. analysed the electrochromic properties.

Funding: This research received no external funding.

Acknowledgments: The authors thank the Ministry of Science and Technology of Republic of China for financially supporting this project.

Conflicts of Interest: The authors declare no conflict of interest.

References

1. Mortimer, R.J. Electrochromic materials. *Annu. Rev. Mater. Res.* **2011**, *41*, 241–268. [[CrossRef](#)]
2. Baetens, R.; Jelle, B.P.; Gustavsen, A. Properties, requirements and possibilities of smart windows for dynamic daylight and solar energy control in buildings: A state-of-the-art review. *Sol. Energy Mater. Sol. Cells* **2016**, *94*, 87–105. [[CrossRef](#)]
3. Camurlu, P.; Gültekin, C.; Bici, Z. Fast switching, high contrast multichromic polymers from alkyl-derivatized dithienylpyrrole and 3,4-ethylenedioxythiophene. *Electrochim. Acta* **2012**, *61*, 50–56. [[CrossRef](#)]
4. Kuo, C.-W.; Wu, B.-W.; Chang, J.-K.; Chang, J.-C.; Lee, L.-T.; Wu, T.-Y.; Ho, T.-H. Electrochromic devices based on poly(2,6-di(9H-carbazol-9-yl)pyridine)-type polymer films and PEDOT-PSS. *Polymers* **2018**, *10*, 604. [[CrossRef](#)]

5. Turkarslan, O.; Ak, M.; Tanyeli, C.; Toppare, L. Enhancing electrochromic properties of conducting polymers via copolymerization: Copolymer of 1-(4-fluorophenyl)-2,5-di(thiophen-2-yl)-1H-pyrrole with 3,4-ethylene dioxythiophene. *J. Polym. Sci. Polym. Chem.* **2007**, *45*, 4496. [[CrossRef](#)]
6. Wu, T.Y.; Li, W.B.; Kuo, C.W.; Chou, C.F.; Liao, J.W.; Chen, H.R.; Tseng, C.G. Study of poly(methyl methacrylate)-based gel electrolyte for electrochromic device. *Int. J. Electrochem. Sci.* **2013**, *8*, 10720–10732.
7. Hsiao, S.-H.; Liao, Y.-C. Facile synthesis of electroactive and electrochromic triptycene poly(ether-imide)s containing triarylamine units via oxidative electro-coupling. *Polymers* **2017**, *9*, 497. [[CrossRef](#)]
8. Nie, G.M.; Zhou, L.J.; Yang, H.J. Electrosynthesis of a new polyindole derivative obtained from 5-formylindole and its electrochromic properties. *J. Mater. Chem.* **2011**, *21*, 13873–13880. [[CrossRef](#)]
9. Hsiao, S.-H.; Lu, H.-Y. Electrosynthesis of aromatic poly(amide-amine) films from triphenylamine-based electroactive compounds for electrochromic applications. *Polymers* **2017**, *9*, 708. [[CrossRef](#)] [[PubMed](#)]
10. Camurlu, P. Polypyrrole derivatives for electrochromic applications. *RSC Adv.* **2014**, *4*, 55832–55845. [[CrossRef](#)]
11. Liu, J.; Mi, S.; Xu, Z.; Wu, J.; Zheng, J.; Xu, C. Solution-processable thiophene-based electrochromic polymers bearing trifluoromethyl rather than long side chains. *Org. Electron.* **2016**, *37*, 169–177. [[CrossRef](#)]
12. Çetin, G.A.; Balan, A.; Durmus, A.; Günbas, G.; Toppare, L. A new p- and n-dopable selenophene derivative and its electrochromic properties. *Org. Electron.* **2009**, *10*, 34–41. [[CrossRef](#)]
13. Yu, W.; Chen, J.; Fu, Y.; Xu, J.; Nie, G. Electrochromic property of a copolymer based on 5-cyanoindole and 3,4-ethylenedioxythiophene and its application in electrochromic devices. *J. Electroanal. Chem.* **2013**, *700*, 17–23. [[CrossRef](#)]
14. Tao, Y.; Zhang, K.; Zhang, Z.; Cheng, H.; Jiao, C.; Zhao, Y. Synthesis, characterizations and electrochromic properties of polymers based on functionalized anthracene. *Chem. Eng. J.* **2016**, *293*, 34–43. [[CrossRef](#)]
15. Hsiao, S.-H.; Liao, W.-K.; Liou, G.-S. Synthesis and electrochromism of highly organosoluble polyamides and polyimides with bulky trityl-substituted triphenylamine units. *Polymers* **2017**, *9*, 511. [[CrossRef](#)]
16. Lu, Q.; Cai, W.; Niu, H.; Wang, W.; Bai, X.; Hou, Y. Novel polyamides with 5H-dibenzo[b,f]azepin-5-yl-substituted triphenylamine: Synthesis and visible-NIR electrochromic properties. *Polymers* **2017**, *9*, 542. [[CrossRef](#)]
17. Guzela, M.; Karatasbz, E.; Ak, M. Synthesis and fluorescence properties of carbazole based asymmetric functionalized star shaped polymer. *J. Electrochem. Soc.* **2017**, *164*, H49–H55. [[CrossRef](#)]
18. Ouyang, M.; Fu, Z.; Lv, X.; Hu, B.; Wang, P.; Huang, S.; Dai, Y.; Zhang, C. A multichromic copolymer based on 4-(9H-carbazol-9-yl)-N,N-diphenylaniline and 3,4-ethylenedioxythiophene prepared via electrocopolymerization. *J. Electrochem. Soc.* **2013**, *160*, H787–H792. [[CrossRef](#)]
19. Feng, F.; Kong, L.; Du, H.; Zhao, J.; Zhang, J. Donor-acceptor-type copolymers based on 3,4-propylenedioxy-thiophene and 5,6-difluorobenzotriazole: Synthesis and electrochromic properties. *Polymers* **2018**, *10*, 427. [[CrossRef](#)]
20. Alkan, S.; Cutler, C.A.; Reynolds, J.R. High-quality electrochromic polythiophenes via BF₃·Et₂O electropolymerization. *Adv. Funct. Mater.* **2003**, *13*, 331–336. [[CrossRef](#)]
21. Welsh, D.M.; Kumar, A.; Morvant, M.C.; Reynolds, J.R. Fast electrochromic polymers based on new poly(3,4-alkylenedioxythiophene) derivatives. *Synth. Met.* **1999**, *102*, 967–968. [[CrossRef](#)]
22. Heydari Gharahcheshmeh, M.; Gleason, K.K. Device fabrication based on oxidative chemical vapor deposition (oCVD): Synthesis of conducting polymers and related conjugated organic materials. *Adv. Mater. Interfaces* **2019**, *6*, 1801564. [[CrossRef](#)]
23. Brooke, R.; Cottis, P.; Talemi, P.; Fabretto, M.; Murphy, P.; Evans, D. Recent advances in the synthesis of conducting polymers from the vapour phase. *Prog. Mater. Sci.* **2017**, *86*, 127. [[CrossRef](#)]
24. Su, Y.-S.; Wu, T.-Y. Three carbazole-based polymers as potential anodically coloring materials for high-contrast electrochromic devices. *Polymers* **2017**, *9*, 284. [[CrossRef](#)]
25. Welsh, D.M.; Kumar, A.; Meijer, E.W.; Reynolds, J.R. Enhanced contrast ratio and rapid switching in electrochromics based on poly(3,4-propylenedioxythiophene) derivatives. *Adv. Mater.* **1999**, *11*, 1379–1382. [[CrossRef](#)]
26. Kuo, C.W.; Chen, B.K.; Li, W.B.; Tseng, L.Y.; Wu, T.Y.; Tseng, C.G.; Chen, H.R.; Huang, Y.C. Effects of supporting electrolytes on spectroelectrochemical and electrochromic properties of polyaniline-poly(styrene sulfonic acid) and poly(ethylenedioxythiophene)-poly(styrene sulfonic acid)-based electrochromic device. *J. Chin. Chem. Soc.* **2014**, *61*, 563–570. [[CrossRef](#)]

27. Kuo, C.-W.; Wu, T.-Y.; Fan, S.-C. Applications of poly(indole-6-carboxylic acid-co-2,2'-bithiophene) films in high-contrast electrochromic devices. *Coatings* **2018**, *8*, 102. [[CrossRef](#)]
28. Ates, M.; Özyılmaz, A.T. The application of polycarbazole, polycarbazole/nanoclay and polycarbazole/Zn-nanoparticles as a corrosion inhibition for SS304 in saltwater. *Prog. Org. Coat.* **2015**, *84*, 50–58. [[CrossRef](#)]
29. Wu, T.Y.; Li, J.L. Electrochemical synthesis, optical, electrochemical and electrochromic characterizations of indene and 1,2,5-thiadiazole-based poly(2,5-dithienylpyrrole) derivatives. *RSC Adv.* **2016**, *6*, 15988–15998. [[CrossRef](#)]
30. Soganci, T.; Soyleyici, H.C.; Ak, M.; Cetisli, H. An amide substituted dithienylpyrrole based copolymer: Its electrochromic properties, physical and analytical electrochemistry, electrocatalysis, and photoelectrochemistry. *J. Electrochem. Soc.* **2016**, *163*, H59–H66. [[CrossRef](#)]
31. Wu, T.-Y.; Su, Y.-S.; Chang, J.-C. Dithienylpyrrole- and tris[4-(2-thienyl)phenyl]amine-containing copolymers as promising anodic layers in high-contrast electrochromic devices. *Coatings* **2018**, *8*, 164. [[CrossRef](#)]
32. Kuo, C.W.; Wu, T.Y.; Huang, M.W. Electrochromic characterizations of copolymers based on 4,4'-bis(*N*-carbazoyl)-1,1'-biphenyl and indole-6-carboxylic acid and their applications in electrochromic devices. *J. Taiwan Inst. Chem. Eng.* **2016**, *68*, 481–488. [[CrossRef](#)]
33. Udum, Y.A.; Hizliateş, C.G.; Ergün, Y.; Toppare, L. Electrosynthesis and characterization of an electrochromic material containing biscarbazole–oxadiazole units and its application in an electrochromic device. *Thin Solid Films* **2015**, *595*, 61–67. [[CrossRef](#)]
34. Koyuncu, S.; Gultekin, B.; Zafer, C.; Bilgili, H.; Can, M.; Demic, S.; Kaya, I.; Icli, S. Electrochemical and optical properties of biphenyl bridged-dicarbazole oligomer films: Electropolymerization and electrochromism. *Electrochim. Acta* **2009**, *54*, 5694–5702. [[CrossRef](#)]
35. Kuo, C.W.; Lee, P.Y. Electrosynthesis of copolymers based on 1,3,5-tris(*N*-carbazoyl)benzene and 2,2'-bithiophene and their applications in electrochromic devices. *Polymers* **2017**, *9*, 518. [[CrossRef](#)] [[PubMed](#)]
36. Wang, B.; Zhao, J.; Liu, R.; Liu, J.; He, Q. Electrosyntheses, characterizations and electrochromic properties of a copolymer based on 4,4'-di(*N*-carbazoyl)biphenyl and 2,2'-bithiophene. *Sol. Energy Mater. Sol. Cells* **2011**, *95*, 1867–1874. [[CrossRef](#)]
37. Kuo, C.W.; Chang, J.K.; Lin, Y.C.; Wu, T.Y.; Lee, P.Y.; Ho, T.H. Poly(tris(4-carbazoyl-9-ylphenyl)amine)/three poly(3,4-ethylenedioxythiophene) derivatives complementary high-contrast electrochromic devices. *Polymers* **2017**, *9*, 543. [[CrossRef](#)]
38. Kuo, C.W.; Wu, T.L.; Lin, Y.C.; Chang, J.K.; Chen, H.R.; Wu, T.Y. Copolymers based on 1,3-bis(carbazol-9-yl)benzene and three 3,4-ethylenedioxythiophene derivatives as potential anodically coloring copolymers in high-contrast electrochromic devices. *Polymers* **2016**, *8*, 368. [[CrossRef](#)] [[PubMed](#)]
39. Kuo, C.-W.; Chang, J.-C.; Lee, P.-Y.; Wu, T.-Y.; Huang, Y.-C. Applications of electrochromic copolymers based on tris(4-carbazoyl-9-ylphenyl)amine and bithiophene derivatives in electrochromic devices. *Materials* **2018**, *11*, 1895. [[CrossRef](#)]
40. Wu, T.Y.; Su, Y.S. Electrochemical synthesis and characterization of 1,4-benzodioxan-based electrochromic polymer and its application in electrochromic devices. *J. Electrochem. Soc.* **2015**, *162*, G103–G112. [[CrossRef](#)]
41. Kuo, C.W.; Hsieh, T.H.; Hsieh, C.K.; Liao, J.W.; Wu, T.Y. Electrosynthesis and characterization of four electrochromic polymers based on carbazole and indole-6-carboxylic acid and their applications in high-contrast electrochromic devices. *J. Electrochem. Soc.* **2014**, *161*, D782–D790. [[CrossRef](#)]
42. Su, Y.S.; Chang, J.C.; Wu, T.Y. Applications of three dithienylpyrroles-based electrochromic polymers in high-contrast electrochromic devices. *Polymers* **2017**, *9*, 114. [[CrossRef](#)] [[PubMed](#)]

